Supporting Information

For

Degradable Polyurethane with Poly(2-ethyl-2-oxazoline) Brushes for Protein Resistance

Jinxian Yang,[a] Lianwei Li,[a] Chunfeng Ma,[b] Xiaodong Ye*[a]

a) Hefei National Laboratory for Physical Sciences at the Microscale, Department of Chemical Physics, University of Science and Technology of China, Hefei, Anhui 230026, China;

b) Faculty of Materials Science and Engineering, South China University of Technology, Guangzhou 510640, China

**To whom correspondence should be addressed: xdye@ustc.edu.cn*

Table S1. GPC results of PEtOx(OH)$_2$-1K and PU-*g*-PEtOx1K

Samples	M_n (g/mol)	M_w (g/mol)	PDI
PEtOx(OH)$_2$-1K	0.98×10^3	1.17×10^3	1.20
PU	5.59×10^4	1.15×10^5	2.05
PU-*g*-PEtOx1K-0.5	3.06×10^4	3.06×10^4	1.94
PU-*g*-PEtOx1K-0.7	3.49×10^4	6.28×10^4	1.80
PU-*g*-PEtOx1K-0.9	4.27×10^4	8.57×10^4	2.01
PU-*g*-PEtOx1K-1.0	6.26×10^4	1.31×10^5	2.10

Table S2. GPC results of PEtOx(OH)$_2$-2K and PU-*g*-PEtOx2K

Samples	M_n (g/mol)	M_w (g/mol)	PDI
PEtOx(OH)$_2$-2K	2.02×10^3	2.27×10^3	1.12
PU	5.59×10^4	1.15×10^5	2.05
PU-*g*-PEtOx2K-0.5	4.56×10^4	8.03×10^4	1.76
PU-*g*-PEtOx2K-0.7	2.50×10^4	3.95×10^4	1.58
PU-*g*-PEtOx2K-0.9	1.65×10^4	3.06×10^4	1.86
PU-*g*-PEtOx2K-1.0	1.53×10^4	2.71×10^4	1.77

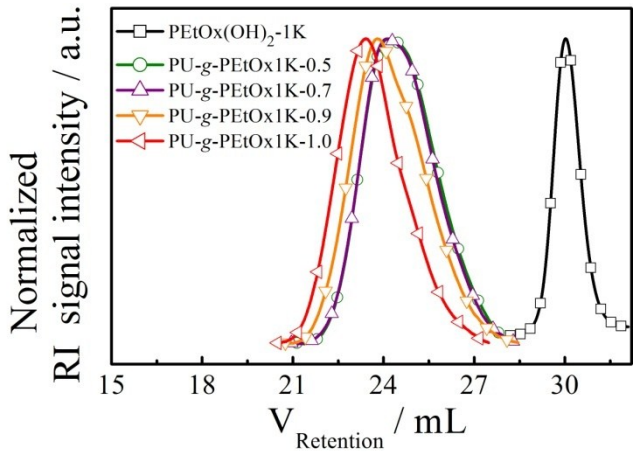

Figure S1. GPC traces from RI detector of PEtOx(OH)$_2$-1K and PU-*g*-PEtOx1K with various graft densities of PEtOx(OH)$_2$-1K.

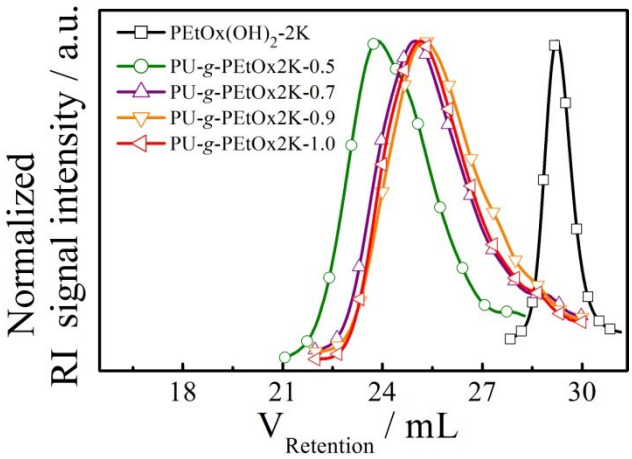

Figure S2. GPC traces from RI detector of PEtOx(OH)$_2$-2K and PU-*g*-PEtOx2K with various graft densities of PEtOx(OH)$_2$-2K.

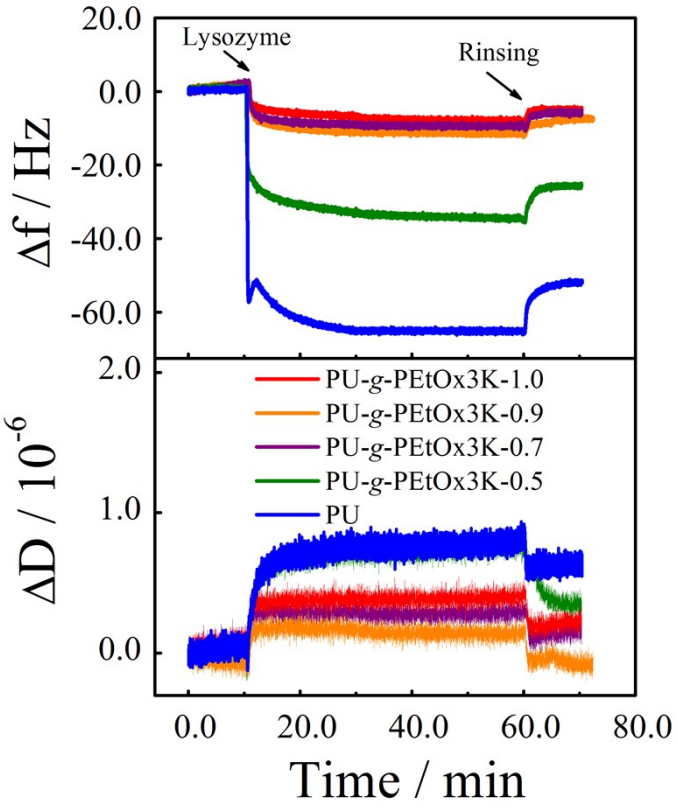

Figure S3. Time dependence of frequency shift (Δf) and dissipation shift (ΔD) for the adsorption of lysozyme on PU-*g*-PEtOx3K surfaces with various graft densities of PEtOx(OH)$_2$-3K at 25 ^{o}C.

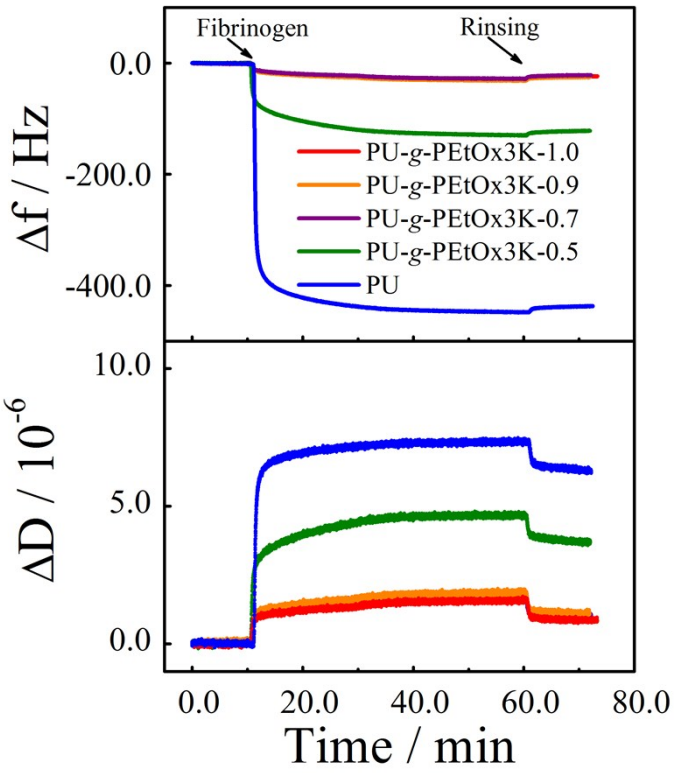

Figure S4. Time dependence of frequency shift (Δf) and dissipation shift (ΔD) for the adsorption of fibrinogen on PU-*g*-PEtOx3K surfaces with various graft densities of $PEtOx(OH)_2$-3K at 25 °C.

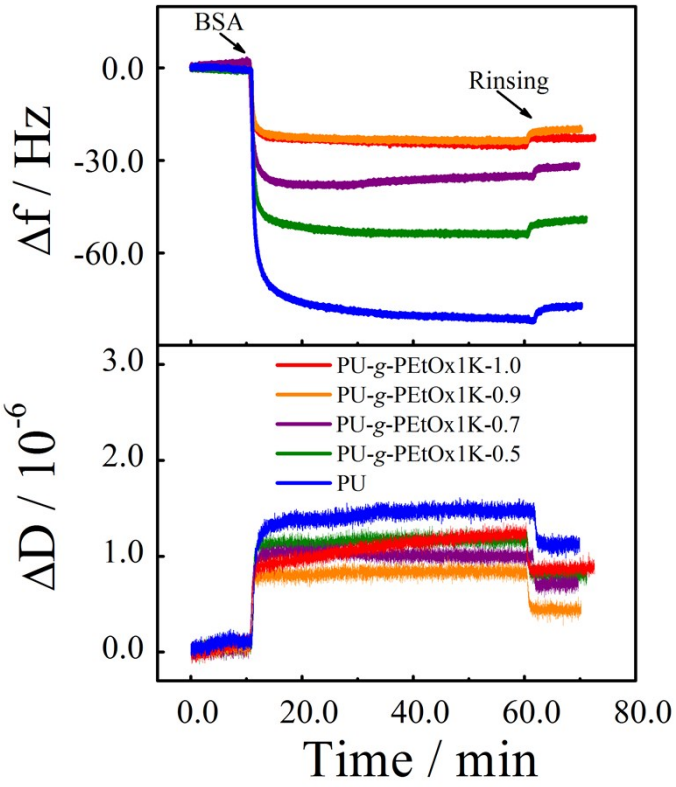

Figure S5. Time dependence of frequency shift (Δf) and dissipation shift (ΔD) for the adsorption of BSA on PU-*g*-PEtOx1K surfaces with various graft densities of $PEtOx(OH)_2$-1K at 25 °C.

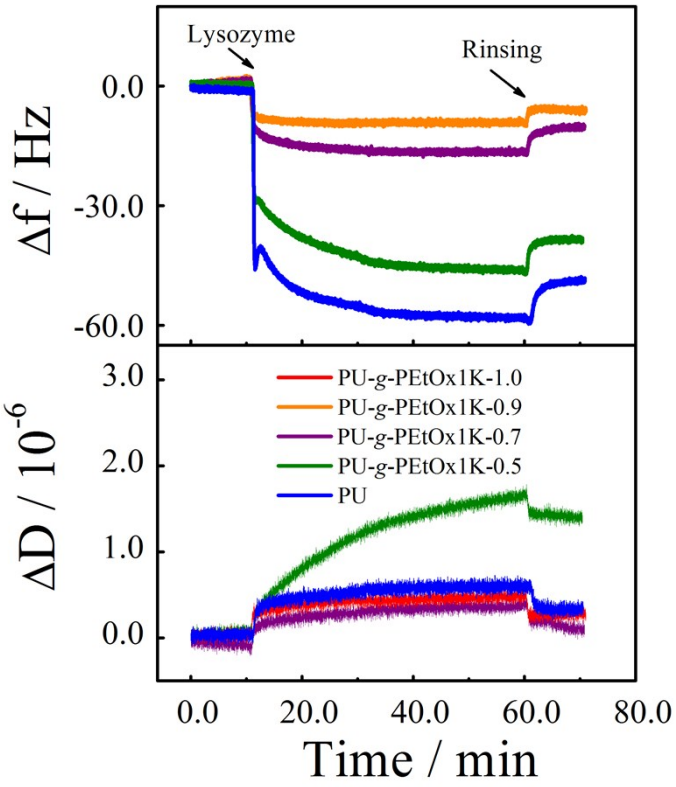

Figure S6. Time dependence of frequency shift (Δf) and dissipation shift (ΔD) for the adsorption of lysozyme on PU-*g*-PEtOx1K surfaces with various graft densities of $PEtOx(OH)_2$-1K at 25 °C.

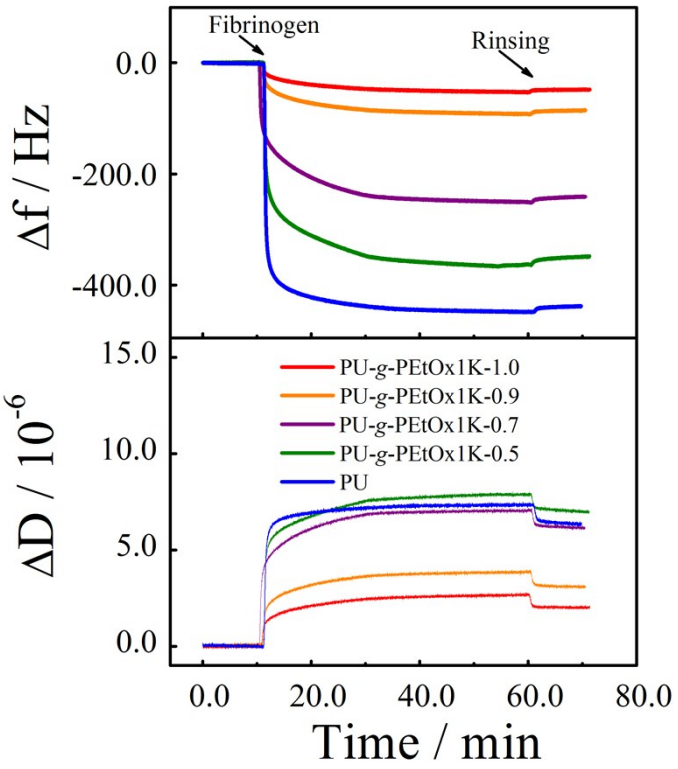

Figure S7. Time dependence of frequency shift (Δf) and dissipation shift (ΔD) for the adsorption of fibrinogen on PU-*g*-PEtOx1K surfaces with various graft densities of $PEtOx(OH)_2$-1K at 25 °C.

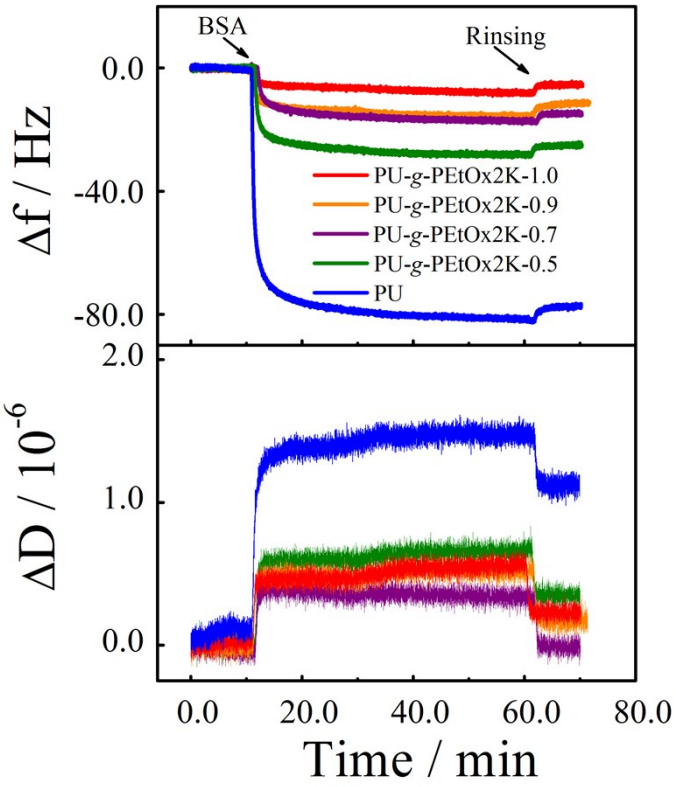

Figure S8. Time dependence of frequency shift (Δf) and dissipation shift (ΔD) for the adsorption of BSA on PU-*g*-PEtOx2K surfaces with various graft densities of $PEtOx(OH)_2$-2K at 25 °C.

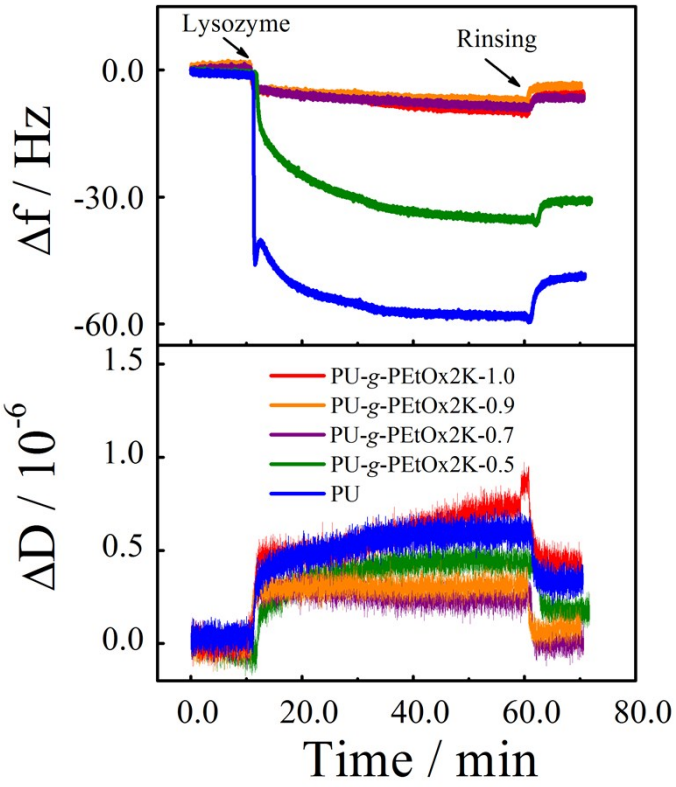

Figure S9. Time dependence of frequency shift (Δ*f*) and dissipation shift (Δ*D*) for the adsorption of lysozyme on PU-*g*-PEtOx2K surfaces with various graft densities of $PEtOx(OH)_2$-2K at 25 °C.

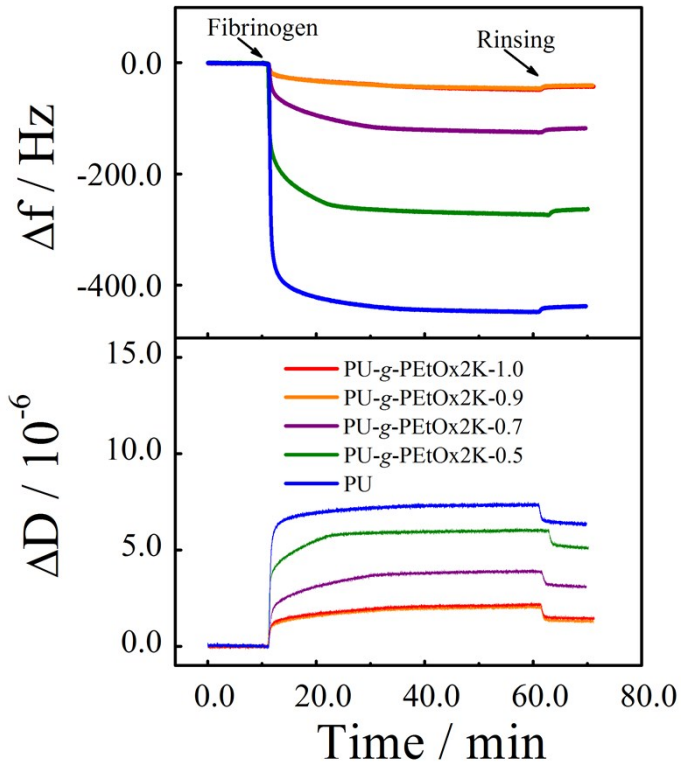

Figure S10. Time dependence of frequency shift (Δf) and dissipation shift (ΔD) for the adsorption of fibrinogen on PU-*g*-PEtOx2K surfaces with various graft densities of $PEtOx(OH)_2$-2K at 25 °C.

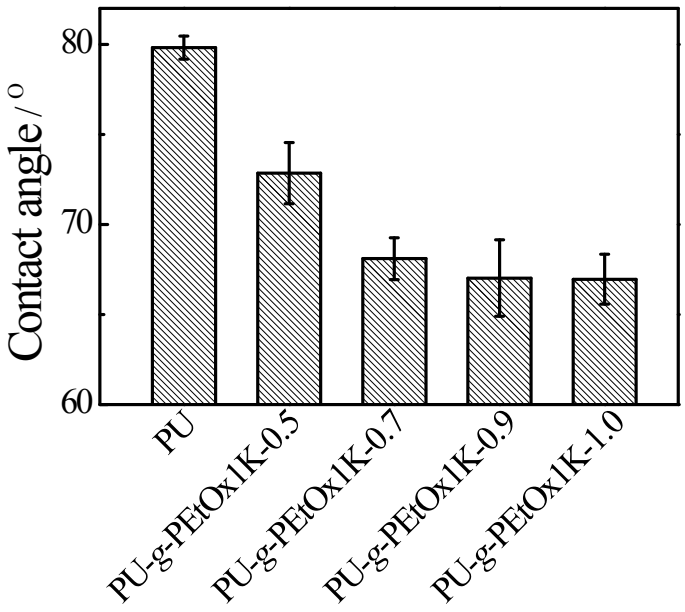

Figure S11. Stationary water contact angle of PU and PU-*g*-PEtOx1K with various graft densities where the $PEtOx(OH)_2$-1K was employed.

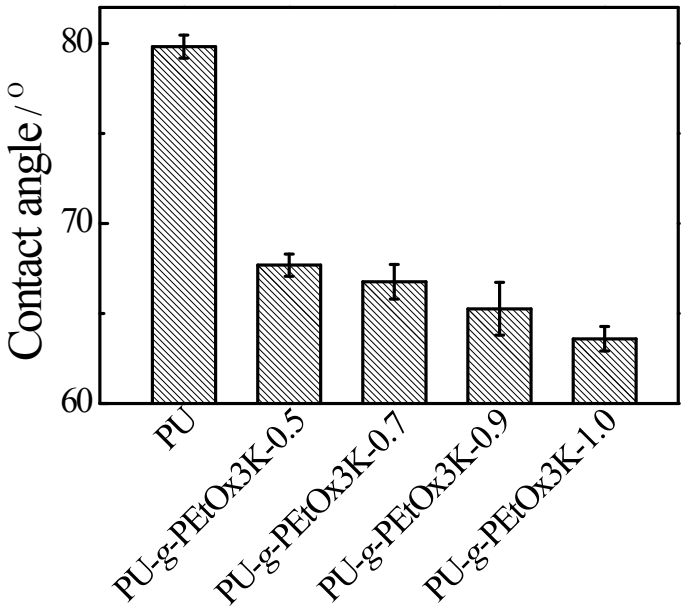

Figure S12. Stationary water contact angle of PU and PU-*g*-PEtOx3K with various graft densities where the $PEtOx(OH)_2$-3K was employed.